Floquet-Liouville approach for calculating Stark profiles in plasmas in the presence of a strong oscillating field

P. Sauvan[1] and E. Dalimier[2]

[1]*Departamento de Ingeniería Energética, ETS Ingenieros Industriales, UNED, C/Juan del Rosal 12, 28040 Madrid, Spain*

[2]*Physique Atomique dans les Plasmas Denses, LULI UMR 7605, CNRS–CEA–École Polytechnique–Université Paris 6, UPMC case 128, 4 Place Jussieu, 75252 Paris Cedex 05 and 91128 Palaiseau, France*

(Received 10 October 2008; revised manuscript received 12 December 2008; published 20 March 2009)

The formalism for the calculation of Stark line profiles in hot dense plasmas submitted to a strong oscillating field is extensively developed. The Liouville space, usually used to deal with the calculation of Stark profiles in dense plasmas, and the Floquet theory, developed to solve time-periodic problems, have been joined together to solve the time-dependent Liouville equation in the so-called Floquet-Liouville formalism. The strong-oscillating-field spectroscopic signatures and their error estimations are discussed for hydrogen- and heliumlike aluminum lines.

DOI: 10.1103/PhysRevE.79.036405 PACS number(s): 52.38.−r, 32.70.−n, 52.70.−m, 32.60.+i

I. INTRODUCTION

The interaction of a laser-produced plasma with a strong oscillating electric field has been studied for many years [1]. The spectroscopic signatures of this strong electric field, produced either by an intense laser pulse of frequency ω_L or by Langmuir oscillations of frequency ω_{pe} (electronic plasma frequency), can be observed on the line shape as dips [2–4] or satellites [5,6]. As for plasmas produced by long-pulse lasers, the alteration of the emitted line shapes by the Langmuir oscillations occurs during the pulse. For laser plasmas generated by high-powered short pulses, the hot dense plasma does exist when the laser is off [7], and, therefore, this laser will not affect the lines emitted from this radiating plasma. Hence, in order to create a strong oscillating electric field interacting with a preformed plasma, a second delayed short-pulse laser has to be used. We address our work to such experimental issues, where the strong oscillating field due to the second laser will modify the Stark profiles.

Oks [8] and Alexiou [9] were the first to work on this topic. They used the wave functions basis of the "dressed atom" [10] to take into account the coupling between the atom states and the oscillating field. The resulting effective radiating system is then submitted to the ion and electron microfields treated as stochastic perturbations, as usual in standard line broadening theories. In these works, the effect of the oscillating field on the interaction of the emitter with the plasma is then treated. As we will see, in the work presented here, we use implicitly dressed emitter states including the static ionic interaction, and only the electron microfield is treated as a stochastic perturbation.

Later Peyrusse [11] proposed another formulation, for Lyman lines. In his work, a nonperturbative treatment of the oscillating field interaction with an emitter submitted to an ionic microfield was developed using Floquet theory [12,13]. The effect of the free-electron interaction was then taken into account as a perturbation. In the work reported in the present paper, we extend Peyrusse's development to a more general formalism for the calculation of the line shapes involved in the emission of plasmas interacting with a strong monochromatic oscillating field with a linear polarization. This task is performed by reformulating the Floquet theory, previously in a Hamiltonian formulation [11], into a Liouvillian one [14], which is better adapted for line shape calculation involving the dynamical evolution of a great number of atomic states. This formulation, well known in mathematical computing of deterministic dynamical systems, is highly efficient in atomic spectroscopy for the evolution of the multistate system density matrix.

In fact, the presence of the strong electric field in the plasma will introduce not only a coupling with the emitters perturbed by the plasma, as described above, but also a coupling with the ion and electron perturbers. More precisely, this last coupling will modify the thermal properties of the plasma (electron velocity distribution, electronic temperature, ionic populations, etc.) leading to a change in the microfield distributions. In other words, the oscillating field has two effects on the emission of a radiator surrounded by a plasma: first, the alteration of the plasma-radiation interaction itself and, second, the alteration of the perturber distributions to be used in the spectral line broadening process. In Oks's, Alexiou's, and Peyrusse's work [8,9,11], just as in the present contribution, this second effect is not taken into account.

As for the second effect evoked above, the modifications of the plasma properties will consist essentially in the electronic distributions of velocity [15], leading for example to a modification of the laser absorption coefficient [16], or to a modification of the collisional rates [17] in atomic kinetics. When all these modifications are taken into account, the results of our work will essentially be affected by the modification of the electron broadening operator due to the anisotropy and the non-Maxwellian distribution of the electron velocity. For a strongly coupled plasma, the electron broadening operator, consistent with the presence of the oscillating field in the plasma, could be obtained, for instance, by using molecular dynamic simulations, involving all interactions between ions and electrons in the plasma, plus all interactions with the strong oscillating field. Simulations have been performed for computing the electronic broadening in strongly coupled plasmas, not submitted to an oscillating field [18,19]. To close this discussion, which offers further oppor-

tunities, we recall that, in the present work, we use the conventional electron broadening operator [20].

After a description of the Floquet-Liouville formalism for the Stark profile (Sec. II), the detailed line shape in plasmas submitted to strong oscillating fields is analyzed as well as the accuracy of the simulations (Sec. III). Finally, in Sec. IV, the strong-oscillating-field spectroscopic signatures and their error estimations are discussed for hydrogen- and heliumlike aluminum lines emitted in recent laser-plasma experiments.

II. FLOQUET-LIOUVILLE FORMALISM

A. Stark line shape in the Liouville formalism

The calculation of Stark profiles within the Liouville formalism is well known [21] and extensively used [22–24]. The starting point of the line shape calculation is the determination of the dipole correlation function [14]

$$C(t) = \mathrm{Tr}[\boldsymbol{d}\boldsymbol{d}(t)\rho], \tag{1}$$

where $\boldsymbol{d}$ is the emitter dipole moment and ρ the density matrix of the emitters and the thermal bath (ions and free electrons). The spectral distribution is then given by the Fourier transform of the dipole correlation function,

$$I(\omega) = \frac{1}{\pi}\,\mathrm{Re}\int_0^\infty e^{i\omega t}C(t)dt. \tag{2}$$

The weak coupling between the emitter and the perturber ions and electrons allows one to write the density matrix ρ as a product form $\rho^{(a)}\rho^{(e)}\rho^{(i)}$, (a), (e), and (i) standing for the emitter, the free electrons and the perturber ions, respectively.

In a first approximation of the Stark formulation, ions are considered as static during the time of interest, and the ionic field, reproducing the global effect of the perturber ion, is then taken constant during the radiative transitions. This field F occurs as a parameter, and the final profile result is an average over the ionic fields, taking into account the ionic field distribution in the plasma. The trace takes care of all transitions involved. The resulting correlation function is

$$C(t) = \int Q(\boldsymbol{F})\mathrm{Tr}_{ae}[\boldsymbol{d}U(\boldsymbol{F},t)(\rho^{(a)}\rho^{(e)}\boldsymbol{d})]d^3\boldsymbol{F}, \tag{3}$$

where $Q(\boldsymbol{F})$ is the ionic microfield distribution function and $U(\boldsymbol{F},t)$ the evolution operator depending parametrically on the microfield value F. After this average over the ionic states, the trace runs only over the emitter and electron states.

The evolution operator $U(\boldsymbol{F},t)$ in the Liouville space satisfies the Schrödinger equation

$$i\frac{dU(\boldsymbol{F},t)}{dt} = L(\boldsymbol{F},t)U(\boldsymbol{F},t), \tag{4}$$

whose solution is

$$U(\boldsymbol{F},t) = \exp\left(-i\int_o^t L(\boldsymbol{F},t')dt'\right). \tag{5}$$

$L(\boldsymbol{F},t)$ is the Liouville operator, which can be expanded as

$$L(\boldsymbol{F},t) = L_a + L_i(\boldsymbol{F}) + L_{of}(t) + L_e(t), \tag{6}$$

where L_a, L_i, L_{of}, and L_e are the Liouville operators for the isolated emitters, and the emitter-ion, emitter–oscillating-field, and emitter–free-electron interactions, respectively.

Following the assumption that the effect of the external field on the free-electron field is neglected, the Liouville operator is expressed as a sum of two Liouville operators: one operating on the emitter states, $L_r(\boldsymbol{F},t)$, and the second only on free-electron states, $L_e(t)$. We obtain

$$L(\boldsymbol{F},t) = L_r(\boldsymbol{F},t) + L_e(t) \tag{7}$$

with $L_r(\boldsymbol{F},t) \equiv L_r(t) = L_a + L_i(\boldsymbol{F}) + L_{of}(t)$.

The trace over the emitter and electron states in (3) can then be expressed as

$$\mathrm{Tr}_{ae}\left[\boldsymbol{d}\exp\left(-i\int_o^t (L_r(\boldsymbol{F},t') + L_e(t'))dt'\right)(\rho^{(a)}\rho^{(e)}\boldsymbol{d})\right]. \tag{8}$$

Because the trace over electron states of the commutator $[L_r, L_e]$ vanishes (i.e., $\mathrm{Tr}_e[[L_r, L_e]] = 0$, because the average over free-electron states does not depend on the radiator states), the trace in the correlation function acts on a product of exponentials, and (8) can be written as

$$\mathrm{Tr}_{ae}\left[\boldsymbol{d}\exp\left(-i\int_o^t L_r(\boldsymbol{F},t')dt'\right)\times\exp\left(-i\int_o^t L_e(t')dt'\right)(\rho^{(a)}\rho^{(e)}\boldsymbol{d})\right] \tag{9}$$

or

$$\mathrm{Tr}_{ae}[\boldsymbol{d}U_r(\boldsymbol{F},t)U_e(t)(\rho^{(a)}\rho^{(e)}\boldsymbol{d})] \tag{10}$$

when using the evolution operators acting on the emitter and the electron states, respectively.

In the impact approximation the trace of the electron evolution operator over electron states can be replaced by a non-Hermitian operator $e^{-\phi_e t}$, where ϕ_e is the electron broadening operator [25,26]. In this context, the trace (10) can now be written as

$$\mathrm{Tr}_a[\boldsymbol{d}U_r(\boldsymbol{F},t)e^{-\phi_e t}(\rho^{(a)}\boldsymbol{d})]. \tag{11}$$

Finally, the correlation function reduces to the trace over emitter states only,

$$C(t) = \int Q(\boldsymbol{F})\mathrm{Tr}_a[\boldsymbol{d}U(\boldsymbol{F},t)(\rho^{(a)}\boldsymbol{d})]d^3\boldsymbol{F}, \tag{12}$$

with the global evolution operator depending on the Liouville operator L_r,

$$U(\boldsymbol{F},t) = \exp\left(-i\int_o^t L_r(\boldsymbol{F},t')dt' - \phi_e t\right) = \exp\left(-i\int_o^t (L_r(\boldsymbol{F},t') - i\phi_e)dt'\right).$$

Introducing the vector notation of the tetradic basis $|\alpha\beta\rangle = |\alpha\rangle \otimes |\beta\rangle$, we can rewrite the trace in (12) as

$$\mathrm{Tr}_a[\boldsymbol{d}U(\boldsymbol{F},t)(\rho^{(a)}\boldsymbol{d})] \equiv \langle \boldsymbol{d}^\dagger | U(\boldsymbol{F},t) | \rho^{(a)}\boldsymbol{d}\rangle \tag{13}$$

where the vectors $|\boldsymbol{d}\rangle$ and $|\rho^{(a)}\boldsymbol{d}\rangle$ are defined as

$$|\boldsymbol{d}\rangle = |\alpha\beta\rangle\langle\alpha|\boldsymbol{d}|\beta\rangle \tag{14}$$

and

$$|\rho^{(a)}\boldsymbol{d}\rangle = |\alpha\beta\rangle \sum_\gamma \langle\alpha|\rho^{(a)}|\gamma\rangle\langle\gamma|\boldsymbol{d}|\beta\rangle. \tag{15}$$

The formalism developed above is identical to the formalism developed in Refs. [14,21]. The only difference is that in our case the Liouville operator is now time dependent and the time integration remains. This is due to the time dependence of the oscillating field.

Since the time dependence in the Liouville operator is periodic, we can use the Floquet theory and replace the time-dependent Liouville formulation by an equivalent time-independent eigenvalue problem.

B. Floquet-Liouville operator

The application of the Floquet theory to solve the time-dependent Schrödinger equation was first formulated by Shirley [12]. Chu and Telnov [13] have published an extended report on the utilization of the Floquet theory for solving quantum problems involving periodic interactions. This technique using quasienergies allows the transformation of the time-dependent differential equation into an infinite eigenvalue problem. The periodic nature of the field interaction provides to the quasienergies and associated states properties useful for the calculation of the evolution operators.

In the previous section, we developed the formalism of the spectral line shape in the Liouville space (using tetradic states $|\alpha\beta\rangle = |\alpha\rangle \otimes |\beta\rangle$). The next step is to formulate the Floquet approach in the Liouville space. The link from the first formalism to the other is straightforward.

In the Liouville space, the global time-dependent Liouville operator has matrix elements given by

$$L_{\alpha\beta,\mu\nu}(t) = H_{\alpha\mu}(t)\delta_{\beta\nu} - H_{\beta\nu}(t)\delta_{\alpha\mu} - i\phi^e_{\alpha\beta,\mu\nu}, \tag{16}$$

where the Hamiltonian H includes ionic Stark interactions and the oscillating field, $\delta_{\alpha\beta}$ is the Kronecker delta function, and $\phi^e_{\alpha\beta,\mu\nu}$ is the electron broadening operator. Invoking the Floquet theory described in the Appendix we can transform the time-dependent Liouville operator into a time-independent Floquet-Liouville operator L_F. This operator satisfies, as demonstrated in [27], an eigenvalue equation involving a matrix of infinite dimension:

$$\sum_{\sigma\tau}\sum_k \langle\alpha\beta;n|L_F|\sigma\tau;k\rangle\langle\sigma\tau;k|\Omega_{\mu\nu,m}\rangle = \Omega_{\mu\nu,m}\langle\alpha\beta;n|\Omega_{\mu\nu,m}\rangle. \tag{17}$$

In (17) $|\Omega_{\mu\nu,m}\rangle$ represents the eigenvector corresponding to the eigenvalue $\Omega_{\mu\nu,m}$, and the states $|\alpha\beta;n\rangle = |\alpha\beta\rangle \otimes |n\rangle$ are expressed in the generalized tetradic Fourier basis. The operator L_F can be written more explicitly as

$$\langle\alpha\beta;n|L_F|\mu\nu;m\rangle = L^{(m-n)}_{\alpha\beta,\mu\nu} + m\omega\delta_{\alpha\mu}\delta_{\beta\nu}\delta_{nm} \tag{18}$$

with

$$L^{(k)}_{\alpha\beta,\mu\nu} = H^{(k)}_{\alpha\mu}\delta_{\beta\nu} - H^{(k)}_{\beta\nu}\delta_{\alpha\mu} - i\phi^{el}_{\alpha\beta,\mu\nu}\delta_{k0}, \tag{19}$$

$$H^{(k)}_{\alpha\beta} = H_{\alpha\beta}\delta_{k,0} + V_{\alpha\beta}(\delta_{k,1} + \delta_{k,-1}), \tag{20}$$

$$H_{\alpha\beta} = E_\alpha\delta_{\alpha\beta} - \langle\alpha|\boldsymbol{d}\cdot\boldsymbol{F}|\beta\rangle, \tag{21}$$

$$V_{\alpha\beta} = -\frac{1}{2}\langle\alpha|\boldsymbol{d}\cdot\boldsymbol{E}|\beta\rangle. \tag{22}$$

In these expressions $H_{\alpha\beta}$ is the ionic Stark Hamiltonian, and $V_{\alpha\beta}$ the interaction with the oscillating field. $\boldsymbol{d}$ is the dipole moment of the emitter and $\boldsymbol{F}$ and $\boldsymbol{E}$ are the intensity of the ionic microfield and of the oscillating field, respectively.

The term $V_{\alpha\beta}(\delta_{k,1}+\delta_{k,-1})$ in Eq. (20) comes from the scalar product $\langle\alpha,n|-\boldsymbol{d}\cdot\boldsymbol{E}\cos\omega t|\beta,m\rangle$. In order to evaluate the scalar products in Eqs. (21) and (22), we introduce the complex vector basis $\boldsymbol{e}_0=\boldsymbol{e}_z$, $\boldsymbol{e}_1=-(1/\sqrt{2})(\boldsymbol{e}_x+i\boldsymbol{e}_y)$, $\boldsymbol{e}_{-1}=(1\sqrt{2})(\boldsymbol{e}_x - i\boldsymbol{e}_y)$, taking the electric field oscillations along the z axis, i.e., $\boldsymbol{d}\cdot\boldsymbol{E}=d_0E$. The ionic microfield $\boldsymbol{F}$ may have any orientation with respect to the oscillating field $\boldsymbol{E}$, so that the scalar product in (21) will be expressed as

$$\boldsymbol{d}\cdot\boldsymbol{F} = d_0F_0 - d_1F_{-1} - d_{-1}F_1, \tag{23}$$

where $F_{0,\pm1}$ has been defined as

$$F_0 = F_z, \quad F_1 = -\frac{1}{\sqrt{2}}(F_x + iF_y), \quad F_{-1} = \frac{1}{\sqrt{2}}(F_x - iF_y). \tag{24}$$

The vector $\boldsymbol{F}$ can be decomposed into parallel and perpendicular components with respect to the oscillating field. Each microfield component can then be written as

$$F_0 = F_\parallel, \quad F_1 = -\frac{1}{\sqrt{2}}F_\perp e^{i\varphi}, \quad F_{-1} = \frac{1}{\sqrt{2}}F_\perp e^{-i\varphi}. \tag{25}$$

Due to the z-axis rotation invariance, one can choose $\varphi=0$.

All these notations introduced in the matrix elements (21) and (22) lead to

$$H_{\alpha\beta} = E_\alpha\delta_{\alpha\beta} - \langle\alpha|d_0|\beta\rangle F_\parallel + \langle\alpha|d_1|\beta\rangle\frac{F_\perp}{\sqrt{2}} - \langle\alpha|d_{-1}|\beta\rangle\frac{F_\perp}{\sqrt{2}} \tag{26}$$

and

$$V_{\alpha\beta} = -\frac{1}{2}\langle\alpha|d_0|\beta\rangle E. \tag{27}$$

The matrix (18) has the same periodic properties as in the Floquet-Hamiltonian formulation:

$$\Omega_{\mu\nu,m+k} = \Omega_{\mu\nu,m} + k\omega, \tag{28}$$

$$\langle\alpha\beta;n+k|\Omega_{\mu\nu,m+k}\rangle = \langle\alpha\beta;n|\Omega_{\mu\nu,m}\rangle. \tag{29}$$

Due to the non-Hermitian nature of L_F, there exists a biorthogonal relationship between left and right eigenvectors,

$$\langle \Omega^{-1}_{\mu\nu,m}|\Omega_{\alpha\beta,n}\rangle = \delta_{\alpha\mu}\delta_{\beta\nu}\delta_{nm}, \tag{30}$$

where $\langle \Omega^{-1}_{\mu\nu,m}|$ and $|\Omega_{\alpha\beta,n}\rangle$ are left and right eigenvectors. From this property, we deduce

$$\langle \Omega^{-1}_{\mu\nu,m}|L_F = \Omega_{\mu\nu,m}\langle \Omega^{-1}_{\mu\nu,m}| \Leftrightarrow L_F^{\dagger}|\Omega^{-1}_{\mu\nu,m}\rangle = \Omega^{-1}_{\mu\nu,m}|\Omega^{-1}_{\mu\nu,m}\rangle \tag{31}$$

and as consequence

$$\Omega^{-1}_{\mu\nu,m} = \Omega^{*}_{\mu\nu,m}. \tag{32}$$

C. Determination of the evolution operator in the Floquet-Liouville formalism

Starting from Shirley's formulation [12], the evolution equation is expressed in the Liouville formulation,

$$i\frac{d}{dt}\rho(t) = L(t)\rho(t) \tag{33}$$

relating the density operator ρ to the evolution operator U,

$$U(t,t_0) = \rho(t)\rho^{-1}(t_0). \tag{34}$$

We then use Floquet's formulation (see the Appendix),

$$\rho(t) = \phi(t)e^{-iQt}, \tag{35}$$

where $\phi(t)$ is a matrix of L_F eigenstates and Q a diagonal matrix, the elements of which are the quasienergies $\Omega_{\alpha\beta,n}$.

The density operator (35) can be written

$$\rho(t) = \sum_{\alpha\beta,n}\sum_{\mu\nu,m}|\alpha\beta;n\rangle\langle\alpha\beta;n|\Omega_{\mu\nu,m}\rangle\langle\Omega_{\mu\nu,m}|e^{-i\Omega_{\mu\nu,m}t}. \tag{36}$$

Taking into account the periodic property (29) and the biorthogonal relationship (30), one can write (36) as

$$\rho(t) = \sum_{\alpha\beta,n}\sum_{\mu\nu}|\alpha\beta;n\rangle\langle\alpha\beta;n|\Omega_{\mu\nu,0}\rangle\langle\Omega_{\mu\nu,0}|e^{-i\Omega_{\mu\nu,0}t} \tag{37}$$

and

$$\rho^{-1}(t) = \sum_{\alpha\beta,n}\sum_{\mu\nu}|\Omega^{-1}_{\mu\nu,0}\rangle\langle\Omega^{-1}_{\mu\nu,0}|\alpha\beta;n\rangle\langle\alpha\beta;n|e^{i\Omega_{\mu\nu,0}t}. \tag{38}$$

The evolution operator (34) then becomes

$$U(t,t_0) = \sum_{\substack{\alpha\beta\\ n}}\sum_{\mu\nu}\sum_{\substack{\gamma\delta\\ l}}|\alpha\beta;n\rangle\langle\alpha\beta;n|\Omega_{\gamma\delta,l}\rangle\langle\Omega^{-1}_{\gamma\delta,l}|\mu\nu;0\rangle \times\langle\mu\nu;0|e^{-i\Omega_{\gamma\delta,l}(t-t_0)}. \tag{39}$$

Since $|\Omega_{\gamma\delta,l}\rangle$ forms a complete basis, we can write the evolution operator (39) more compactly,

$$U(t,t_0) = \sum_{\substack{\alpha\beta\\ n}}\sum_{\mu\nu}|\alpha\beta;n\rangle\langle\alpha\beta;n|\exp[-iL_F(t-t_0)]|\mu\nu;0\rangle \times\langle\mu\nu;0|, \tag{40}$$

and consequently its matrix elements,

$$U_{ab,a'b'}(t,t_0) = \sum_n \langle ab;n|\exp[-iL_F(t-t_0)]|a'b';0\rangle e^{in\omega_L t}, \tag{41}$$

where we have written

$$\langle ab|\alpha\beta;n\rangle = \langle ab|\alpha\beta\rangle\otimes|n\rangle \equiv \langle ab|\alpha\beta\rangle e^{in\omega_L t}. \tag{42}$$

In Eq. (41), the periodic property of the eigenvector allowed the removal of the sum over $|m\rangle$ states, and the setting of the state $|m\rangle=|0\rangle$, arbitrarily.

We see in Eq. (41) that the evolution operator is defined on the tetradic basis $|\alpha\beta\rangle$, and the Floquet-Liouville operator is defined on an infinite generalized tetradic Fourier basis $|\alpha\beta;n\rangle$. The reduction of the tetradic Fourier basis $|\alpha\beta;n\rangle$ to the tetradic basis $|\alpha\beta\rangle$ is performed by summing over all projections of the Floquet-Liouville operator on the subspace with a fixed mode n.

In Sec. II A, when we averaged over electron states and defined a time-independent electron broadening operator, we averaged over all initial times, taking into account only the difference $t-t_0$ [25]. Introducing the new variable $s=t-t_0$, we can express the time evolution operation in terms of initial time and elapsed time s as

$$U_{\alpha\beta,\mu\nu}(s,t_0) = \sum_n \langle\alpha\beta;n|\exp(-iL_F s)|\mu\nu;0\rangle e^{in\omega_L s}e^{in\omega_L t_0}. \tag{43}$$

The time-averaged evolution operator is then obtained by integration over all initial times t_0, keeping constant the interval s:

$$\bar{U}_{\alpha\beta,\mu\nu}(s) = \lim_{\tau\to\infty}\frac{1}{\tau}\int_0^{\tau}\sum_n \langle\alpha\beta;n|\exp(-iL_F s) \times|\mu\nu;0\rangle e^{in\omega_L s}e^{in\omega_L t_0}dt_0. \tag{44}$$

Since the only dependence on t_0 in the integrand is in the exponential, the nonzero contribution will be when $n=0$, and $\bar{U}_{\alpha\beta,\mu\nu}(s)$ takes the form

$$\bar{U}_{\alpha\beta,\mu\nu}(s) = \langle\alpha\beta;0|\exp(-iL_F s)|\mu\nu;0\rangle. \tag{45}$$

Finally, the average over initial time has removed the sum over Fourier modes, and only the mode $n=0$ remains.

We have thus defined all necessary operators to calculate the intensity profile (2).

III. LINE PROFILE DETERMINATION

A. Calculation

The electric dipole moment operator $\boldsymbol{d}$ occurring in Eq. (3), can be decomposed in the vector basis $\boldsymbol{e}_0$, $\boldsymbol{e}_1$, $\boldsymbol{e}_{-1}$, and a correlation function $C_q(t)$ can be associated with each polarization state corresponding to the component q. The resulting intensity for each polarization state will be

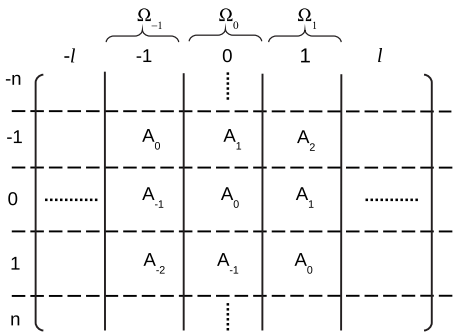

FIG. 1. Structure of the transfer matrix M_p associated with the Floquet-Liouville operator.

$$I_q(\omega) = \frac{1}{\pi} \mathrm{Re} \int_0^\infty e^{i\omega t} C_q(t) dt. \tag{46}$$

Substituting the expression for the component $\phi_q(t)$ we obtain

$$I_q(\omega) = \frac{1}{\pi} \mathrm{Re} \int_0^\infty e^{i\omega t} \int Q(\boldsymbol{F}) \langle d_q^\dagger | U(\boldsymbol{F},t) | \rho^{(a)} d_q \rangle d^3\boldsymbol{F}\, dt, \tag{47}$$

d_q standing for the dipole moment component q.

The two integrations are interchangeable, so that

$$I_q(\omega) = \int Q(\boldsymbol{F}) \left(\frac{1}{\pi} \mathrm{Re} \int_0^\infty e^{i\omega t} \langle d_q^\dagger | U(\boldsymbol{F},t) | \rho^{(a)} d_q \rangle dt \right) d^3\boldsymbol{F}. \tag{48}$$

Expressing the evolution operator in terms of the matrix components of the Floquet-Liouville operator, (48) gives

$$I_q(\omega) = \int Q(\boldsymbol{F}) \times \left(\frac{1}{\pi} \mathrm{Re} \int_0^\infty e^{i\omega t} \langle d_q^\dagger | P_0 \exp(-iL_F t) P_0 | \rho^{(a)} d_q \rangle dt \right) d^3\boldsymbol{F}, \tag{49}$$

where P_0 is the projector on the Floquet subspace $n=0$,

$$P_0 = \sum_{\alpha\beta} |\alpha\beta\rangle\langle\alpha\beta;0|. \tag{50}$$

Equation (49) can be compacted as

$$I_q(\omega) = \int Q(\boldsymbol{F}) J_{q,\boldsymbol{F}}(\omega) d^3\boldsymbol{F}, \tag{51}$$

where $J_{q,\boldsymbol{F}}(\omega) = (1/\pi)\mathrm{Re}\int_0^\infty e^{i\omega t} \langle d_q^\dagger | P_0 \exp(-iL_F t) P_0 | \rho^{(a)} d_q \rangle dt$ represents the line shape in the presence of an oscillating field with a polarization q, and when an ionic field $\boldsymbol{F}$ is perturbing the emitter. $I_q(\omega)$ still depends on the oscillating field.

The presence of the oscillating field introduces a polarization of the space, forcing us to consider the orientation of the ionic microfield with respect to the oscillating field. We have seen in Sec. II B that the relevant ionic field components are

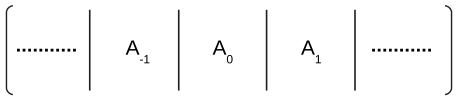

FIG. 2. Projection of the matrix M_p onto the subspace $n=0$.

the parallel and perpendicular ones. Taking into account these two components, within the assumption of an isotropic ionic microfield, (51) may be written as [11]

$$I_q(\omega) = \frac{1}{2} \int_0^\infty W(F) \int_{-1}^1 J_{q,F,\mu}(\omega) d\mu\, dF, \tag{52}$$

where $\mu = \cos\theta$, θ being the angle between the ionic microfield direction and z axis. The parallel and perpendicular components are then $F_\parallel = F\mu$ and $F_\perp = F\sqrt{1-\mu^2}$, where F is the ionic microfield intensity. $W(F)$ represents the distribution function restricted to the ionic microfield intensity.

The Stark effect splits each initial line into several Stark components, on which natural and electronic relaxations act as noise filters [24].

In the following, we discuss the numerical treatment that will condition the accuracy of the line profile calculation. A discretization of the formula (52) leads to a weighted sum as

$$I_q(\omega) = \sum_p W_p J_{q,p}(\omega), \tag{53}$$

where $J_{q,p}(\omega)$ is the line shape function for the discretization abscissa p, for given microfield intensity and direction. The associated weights W_p depend on the ionic microfield distribution and on the discretization method. In fact, it is a double summation, as in (52), that has to be performed hereafter. For this purpose, the weights W_p stand for a product $W_k^{(2)} W_l^{(G)}$, holding all the aspects discussed above. Numerical results have shown that taking Gauss-Legendre quadrature weights $W_l^{(G)}$, with the respective abscissa μ, is a good choice for the angle summation, while two-point integration weights $W_k^{(2)}$, with no constant interval, have to be used, both for performing the integration of the microfield dependence and for optimizing the accuracy of the integration,

$$I_q(\omega) = \sum_{k,l} W_k^{(2)} W_l^{(G)} J_{q,k,l}(\omega). \tag{54}$$

The indices k and l involved in (54) characterize the discretization abscissa values. In (54), as well as in subsequent formulas, it is important to underline that the line shapes are calculated for a fixed oscillating field intensity E.

We now go back to the line shape formulation with the notations introduced in the double integration (52). Following the Calisti *et al.* procedure [24], we diagonalize the Floquet-Liouville operator $L_F(\boldsymbol{F})$ for every value of the index p, i.e., for every F and μ. In this diagonal basis $J_{q,p}(\omega)$ can be written as

$$J_{q,p}(\omega) = \frac{1}{\pi} \mathrm{Re} \int_0^\infty e^{i\omega t} \langle d_q^\dagger | P_0 M_p \exp(-i\Omega_p t) M_p^{-1} P_0 | \rho^{(a)} d_q \rangle dt \tag{55}$$

where $\exp(-i\Omega_p t)$ is a diagonal matrix, the elements of which are quasienergy values, and M_p are transfer matrices from the diagonal basis $|\Omega^{(p)}_{\gamma\delta,l}\rangle$ to the $|\alpha\beta;n\rangle$ basis:

$$M_p = \sum_{\substack{\alpha\beta \\ n}} \sum_{\substack{\gamma\delta \\ l}} |\alpha\beta;n\rangle\langle\alpha\beta;n|\Omega^{(p)}_{\gamma\delta,l}\rangle\langle\Omega^{(p)}_{\gamma\delta,l}|, \tag{56}$$

$$M_p^{-1} = \sum_{\substack{\alpha\beta \\ n}} \sum_{\substack{\gamma\delta \\ l}} |\Omega^{(p)^{-1}}_{\gamma\delta,l}\rangle\langle\Omega^{(p)^{-1}}_{\gamma\delta,l}|\alpha\beta;n\rangle\langle\alpha\beta;n|. \tag{57}$$

The Fourier transform in (55) can be performed easily, and leads to the following form for $J_{q,p}(\omega)$:

$$J_{q,p}(\omega) = -\frac{1}{\pi} \mathrm{Im} \langle d_q^\dagger | P_0 M_p \begin{bmatrix} \ddots & & & \\ & \frac{1}{\omega - \Omega_{\alpha\beta,n}} & & \\ & & \ddots & \\ \frac{1}{\omega - \Omega_{\alpha\beta,0}} & & & \\ & \ddots & & \\ & & \frac{1}{\omega - \Omega_{\alpha\beta,-n}} & \\ & & & \ddots \end{bmatrix} M_p^{-1} P_0 | \rho^{(a)} d_q \rangle. \tag{58}$$

The diagonal matrix in (58) is an infinite matrix in which all Floquet modes n are considered. In the numerical calculation; the infinite dimension of this matrix has to be reduced to a finite number of modes n. As we will see in Sec. III B, the number of mode to be included in the calculation can estimated in order to achieve a desired accuracy.

The expression (58) can be written as

$$J_{q,p}(\omega) = \sum_k \frac{\beta_k(\omega - x_k) + \alpha_k y_k}{(\omega - x_k)^2 + y_k^2}, \tag{59}$$

where x_k and y_k are, respectively, the real and imaginary parts of the eigenvalue Ω_k, and α_k and β_k are the real and imaginary parts of the complex amplitudes depending on the values of M_p, $\mathbf{d}$, and $\rho^{(a)}$.

Because of the anisotropy introduced by the oscillating field in the given direction, the observed profile will depend on the direction of the observation axis with respect to the field direction. The angle-dependent profile is then given by [11]

$$\varphi(\omega,\theta) = \Phi_\parallel(\omega)\cos^2\theta + \Phi_\perp(\omega)\sin^2\theta, \tag{60}$$

where θ is the angle of observation with respect to the oscillating field axis, and $\Phi_\parallel(\omega)$ and $\Phi_\perp(\omega)$ are the parallel and transverse profiles observed, i.e., in the field direction and in the orthogonal direction, respectively. These profiles are expressed in terms of the polarized radiations f_1, f_{-1}, and f_0 (corresponding to the electric dipole moment components) as $\Phi_\parallel(\omega) = \frac{1}{2}(f_1 + f_{-1})$ and $\Phi_\perp(\omega) = \frac{1}{4}(f_1 + f_{-1}) + \frac{1}{4}f_0$.

B. Truncation error estimation

As seen in the previous sections, the Floquet-Liouville operator, introduced to solve the time-dependent problem (Stark effect in a time-dependent external field) leads to a time-independent treatment carried out thanks to an operator with an infinite dimension. Nevertheless, the periodic property of this operator allows one to consider only the projection of the Floquet-Liouville operator on the Floquet subspace n.

The periodic property of the Floquet-Liouville operator is highlighted in Fig. 1 through the transfer matrix M_p. This matrix can be decomposed into a block square matrix A (the Floquet mode and the eigenvalue being fixed), the dimension of which is the dimension of the tetradic basis $|\alpha\beta\rangle$. Each block column represents the set of eigenvectors associated with the eigenvalues $\Omega_{\gamma\delta,l}$ with a given Floquet mode value. The horizontal block lines delimit the Floquet subspace in which the components of the eigenvectors belong. We see therefore on Fig. 1 that the components corresponding to the subspace $n=0$ of the eigenvectors associated to the eigenvalues $l=0$ are equal to the components corresponding to the subspace $n=1$ of the eigenvectors associated to the eigenvalue $l=1$.

More generally the relation between components and eigenvectors is that all matrices $A_{(l-n)}$, representing the components corresponding to the subspace n of the eigenvectors associated with the eigenvalue l, are equal if the differences $l-n$ are equal. The result of the product $P_0 M_p$ is the projection of the matrix M_p onto the subspace $n=0$, as shown on Fig. 2.

Depending on the coupling values between the Floquet subspaces for the Floquet-Liouville operator, there will exist a value of n for which the matrices A_m, $|m|>|n|$, are negligible. For instance, if there is no coupling between Floquet subspaces, i.e., if there is no oscillating field, the only nonzero matrix will be the A_0 matrix. The role of this truncation of the Floquet subspace for controlling the precision of the line shape is explained progressively in what follows.

As shown in Fig. 2, the left and right sides of the matrix P_0M are formed by matrices A_n and A_{-n} with $n\to\infty$. We will demonstrate that we can choose a value of n for which the matrix A_m ($|m|>|n|$) is negligible, reducing as a consequence the number of Floquet modes to be involved in the calculation of the profiles.

$$F=\begin{bmatrix}
\ddots & & & & & & & \\
 & \omega_{\alpha\beta}-n\omega & V & & & & & \\
 & V & \omega_{\alpha\beta}-\omega & V & & & & \\
 & & V & \omega_{\alpha\beta} & V & & & \\
 & & & V & \omega_{\alpha\beta}+\omega & V & & \\
 & & & & V & \omega_{\alpha\beta}+n\omega & & \\
 & & & & & & \ddots &
\end{bmatrix},$$

where $\omega_{\alpha\beta}$ stands for the averaged transition energy and V for the interaction of the emitter with the field. As for the Floquet-Liouville matrix, the number of columns and rows is $2n+1$ when considering n modes for the oscillating field.

This matrix can be transformed as $G=(1/\omega)(F-\omega_{\alpha\beta}I)$, where I stands for the identity matrix, $\omega_{\alpha\beta}$ and ω being scalar values. The two operators F and G have the same eigenvectors and eigenvalues, these quantities being required for the spectral line shape calculation.

The new matrix G can be written as

$$G=\begin{bmatrix}
\ddots & & & & & & \\
 & -n & u & & & & \\
 & u & -1 & u & & & \\
 & & u & 0 & u & & \\
 & & & u & 1 & u & \\
 & & & & u & n & \\
 & & & & & & \ddots
\end{bmatrix},$$

where $u=V/\omega$. The eigenvalues of the matrix G differ from integers. It is easy to see that "zero" is a particular eigenvalue. The eigenvector corresponding to the zero eigenvalue has the following components:

We can have an estimation of this mode number if we consider the tridiagonal block form of the Floquet-Liouville operator (Fig. 8 below). We make the assumption that the block matrix can be reduced to a scalar value by averaging the most significant values of the matrix. More precisely we can take for the diagonal blocks the average of diagonal elements, and for the nondiagonal blocks the element with the highest absolute value.

We will now go further for the estimation of the precision of the oscillating field effect when the Stark interaction is neglected. Considering only the effect of the oscillating field, the tridiagonal operator has the structure

$$X=\begin{bmatrix}
\vdots \\
-a_2 \\
-a_1 \\
a_0 \\
a_1 \\
a_2 \\
\vdots
\end{bmatrix}.$$

Setting $a_0=1$, the coefficients a_n are solutions of the system $AY=B$, with

$$A=\begin{bmatrix}
1 & u & & \\
u & 2 & u & \\
 & u & 3 & \\
 & & & \ddots
\end{bmatrix},\quad Y=\begin{bmatrix}
a_1 \\ a_2 \\ a_3 \\ \vdots
\end{bmatrix},\quad B=\begin{bmatrix}
-u \\ 0 \\ 0 \\ \vdots
\end{bmatrix}.$$

If we cut the matrix A to the dimension m (m will correspond to the number of modes to consider), the value of the last component a_m of the vector Y is

$$a_m=\frac{u^m}{C_m} \tag{61}$$

with

$$C_m = \sum_{k=0}^{\mathrm{int}(m/2)} (-1)^{k+m} \alpha_k^m \frac{(n-k)!}{k!} u^{2k}. \quad (62)$$

In the formula α_k^m are given by the recurrence relation $\alpha_k^m = \alpha_k^{m-1} + \alpha_{k-1}^{m-2}$. The range of k is $0 \leqslant k \leqslant \mathrm{int}(m/2)$ with $\alpha_0^m = 1$ and $\alpha_1^m = m-1$. Thus we have demonstrated that the number of modes m to consider for getting a desired precision in the line shape calculation is related to the value of the last coefficient a_m.

In the case of $u < 1$ we can easily approximate a_m:

$$a_m \propto (-1)^m \frac{u^m}{m!}, \quad (63)$$

and then evaluate the mode m for which the vector components a_m are negligible. In the case of $u > 1$ the estimation of m is more complicated, and we have to evaluate the coefficients C_m in (62) to determine if a_m is negligible.

As an example, if u is equal to 0.9, the value of the component a_m for $m=6$ is about 10^{-3}, and since $a_0=1$, we have $a_6/a_0 \approx 10^{-3}$, giving the precision connected to the number of modes considered. If u is equal to 2 the value of a_m for $m=9$ is about 2×10^{-3} and we have $a_9/a_0 \approx 2 \times 10^{-3}$.

We have thus obtained a method and defined the algorithm to estimate the number of Floquet modes to involve in the calculation of the line shape in order to achieve the desired accuracy. The number of modes to be considered will depend on the oscillating field intensity and the spectral region of interest. Each mode corresponds to a couple of satellites, located on each side of the central line, at the unperturbed energy $n\hbar\omega_L$ (with respect to the central line). The coupling between modes will then determine the shift and relative intensities of the different satellites.

IV. RESULTS AND DISCUSSION

In this section we present some calculations of spectral profiles of aluminum hydrogenlike and heliumlike lines emitted in hot dense laser plasmas submitted to an external oscillating field. With these results we will pay particular attention to the matrix truncation with respect to the error evaluation and validate the convergence procedure. Finally we will highlight some exotic structures (satellites and dips) in the line profiles emitted in the presence of a strong oscillating field.

A. Error estimation and convergence of the line profile

We present results showing the convergence of the line profile when the number of Floquet modes used increases. We confirm the link of this convergence with the dependence of the error estimation on the number of modes considered.

In Fig. 3 we have calculated the Al He-β line profile emitted by a laser plasma at density N_e 10^{21} cm^{-3} perturbed by an oscillating field (frequency $\hbar\omega_L = 1.54$ eV and intensity $I_L = 5 \times 10^{15}$ W cm^{-2}). Those conditions correspond to recent experiments performed by Renner *et al.* [28]. Figures 3 and 4 correspond to profiles observed in the direction of the oscillating field (parallel profile) and in the transverse direction (perpendicular profile), respectively. In each case the profiles

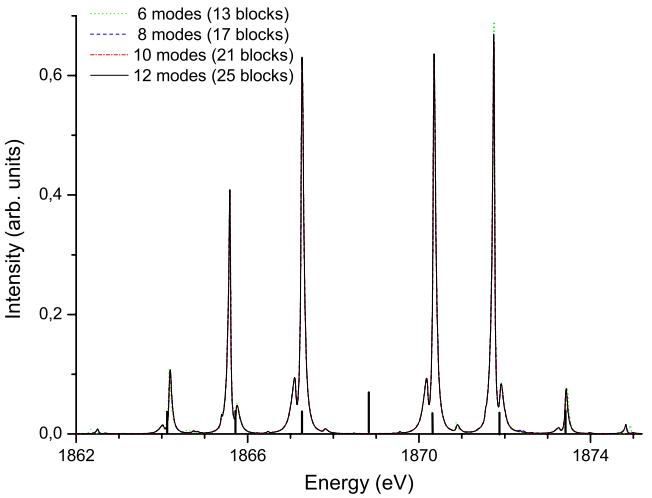

FIG. 3. (Color online) Parallel profiles of the Al He-β line calculated with different numbers of modes. The number of blocks $(2n+1)$ characterizes the dimension of the Floquet matrix. Vertical lines show the $n\hbar\omega_L$ positions with respect to the unperturbed line.

resulting from calculations using 6, 8, 10, and 12 modes have been superimposed. The estimated errors using Eqs. (61) and (62) are given in Table I. These evaluations are obtained when the Stark effect is neglected.

In fact the convergence will depend on the Stark effect and on dipole moment component d_q [see (52) for instance]. For these reasons the convergence criteria will be different for parallel and perpendicular profiles. We see in Figs. 3 and 4 that the parallel profile converges more rapidly than the perpendicular one. For the parallel profile the convergence is reached with six modes, while the perpendicular profile needs about ten modes to have a reliable profile.

B. Line profile calculation

The quasienergies introduced by the Floquet theory presented above are traduced on the line profiles by the presence

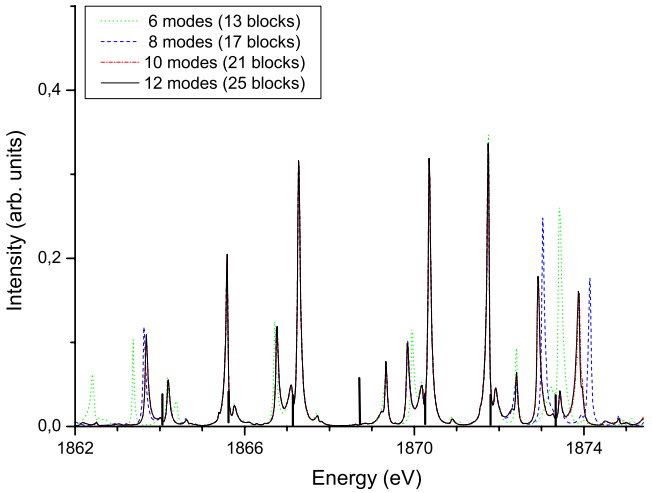

FIG. 4. (Color online) Perpendicular profiles of the Al He-β line calculated with different numbers of modes. The number of blocks $(2n+1)$ characterizes the dimension of the Floquet matrix. Vertical lines show the $n\hbar\omega_L$ positions with respect to the unperturbed line.

TABLE I. Truncation error estimation for the Al He-β profile calculation versus the number of modes used.

Number of modes	Error estimations
6	1×10^{-1}
8	1×10^{-2}
10	5×10^{-4}
12	2×10^{-5}

of satellite transitions corresponding to the Floquet modes. The intensity of those satellites depends on the strength of the coupling between the plasma and the Floquet modes (this coupling depending on the strength of the oscillating field) and their position depends on the field frequency ω_L.

In Fig. 4 concerning Al Ly-α, the fine structure is taken into account, and for this reason the quasienergies and the line profiles are not symmetric. When the ionic microfield is zero ($F=0$) (Fig. 5), we can distinguish the Lyman-α components $2s^{1/2}$, $2p^{1/2}$, and $2p^{3/2}$. The last component $2p^{3/2}$, initially degenerate for the isolated ion, is split into two components due to the presence of the oscillating field E. When the ionic microfield F increases, the quasienergy states come sufficiently close to each other to interact and lead to avoided crossings. The resulting perpendicular and parallel profiles are plotted in Fig. 6.

Finally, we have plotted on Fig. 7 the aluminum He-β line profiles emitted by a near critical plasma perturbed by an oscillating field for four different laser intensities. The perturbing laser wavelength is $\lambda_L=0.53$ μm. The plasma conditions are $N_e=3\times10^{21}$ cm^{-3} and $T_e=150$ eV. The Doppler broadening has been included. The figure shows the evolution of the line profile when the oscillating field intensity increases. At 10^{13} W cm^{-2} [Fig. 7(a)] the profile is not modified by the perturbing oscillating field. On Fig. 7(b) parallel and perpendicular profiles start to differ from each other; we

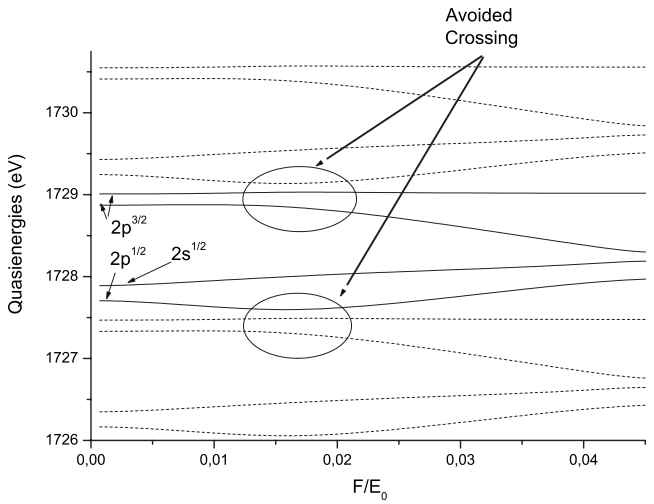

FIG. 5. Quasienergies for the level $n=2$ of the ion Al^{12+} versus the ionic microfield F taken in atomic field units E_0 ($E_0=e/a_0^2=1$ atomic unit). The fundamental level is taken for the energy reference.

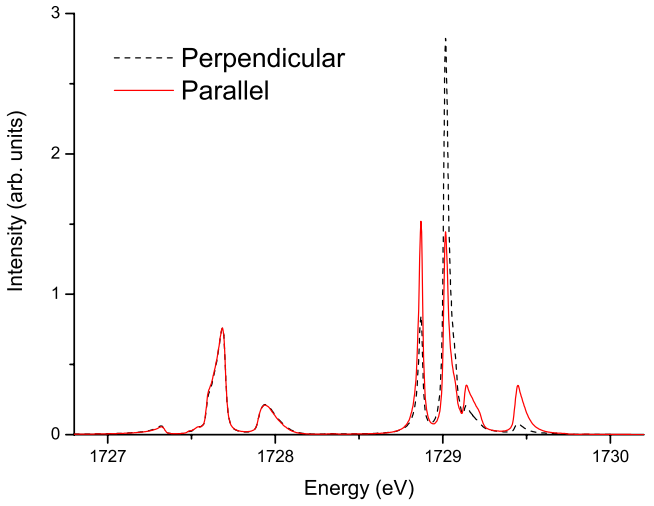

FIG. 6. (Color online) Parallel and perpendicular profiles for the Al Ly-α line with the same conditions (for the plasma and the oscillating field) as for He β (Fig. 3).

can see on the blue wing a satellite emerging. When the intensity becomes higher [Fig. 7(c)] the satellites due to the interaction with the oscillating field grow while the main central line decreases. At very high intensity [Fig. 7(d)], the central part of the line has disappeared and only the satellites at the positions $n\hbar\omega_L$ remain.

V. CONCLUSION

In this work we have described a theoretical formalism for the calculation of the spectral line shapes emitted by hot dense plasma in the presence of a strong oscillating field. The direct coupling between the Stark broadening and the effect of the oscillating field on the emitter is taken into account by the Floquet-Liouville approach. This formalism is highly efficient as it can be directly implemented in any spectral line shape simulation: it can be applied for the spectra of multielectron radiators and not only for hydrogenlike and heliumlike transitions. The introduction of the error estimation, due to the matrix truncation, in the profile calculation, allows the convergence of the profiles to be ensured without computing too many profiles with different numbers of mode. It is also important to underline that, up to now, to our knowledge no heliumlike profile computations have been done in the described conditions.

Finally, we can give as a constructive comment that this formalism could be the starting point for a new formalism devoted to the calculation of the redistribution of the resonance radiation induced by x-ray lasers. This work enhances the advance for the diagnostics of the oscillating laser field from the spectroscopic exotic structures (dips and satellites) and establishes a link between two communities: the laser-plasma interaction and atomic physics in plasmas communities.

ACKNOWLEDGMENT

This work has been supported by INTAS Project No. 06-1000017-9041.

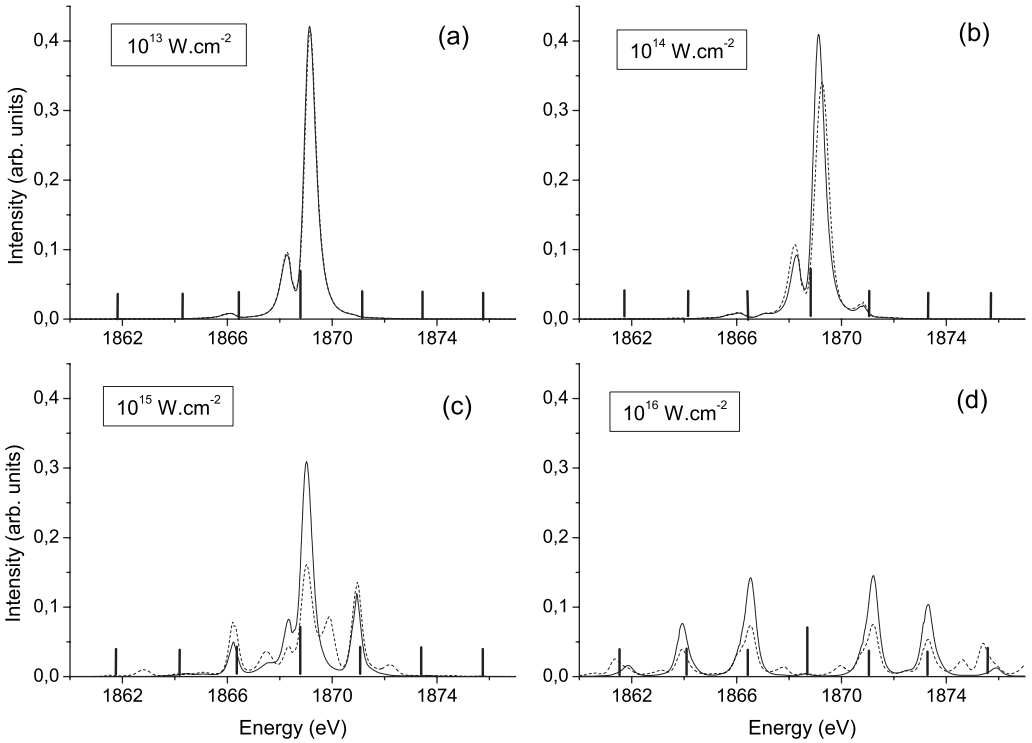

FIG. 7. Parallel and perpendicular profiles for the Al He-β line perturbed by an oscillating field at different oscillating field intensities. Vertical lines show the $n\hbar\omega_L$ positions with respect to the unperturbed line. Parallel and perpendicular profiles are plotted with solid and dashed lines, respectively.

APPENDIX

1. General properties of the Floquet states

Let us consider a quantum system driven by a periodic external field with a frequency ω. The time-dependent Schrödinger equation of this system is ($\hbar=1$)

$$H(\boldsymbol{r},t)\psi(\boldsymbol{r},t) = i\frac{\partial}{\partial t}\psi(\boldsymbol{r},t). \tag{A1}$$

The Hamiltonian can be divided into two parts

$$H(\boldsymbol{r},t) = H_0(\boldsymbol{r}) + V(\boldsymbol{r},t). \tag{A2}$$

$H_0(\boldsymbol{r})$ is the unperturbed Hamiltonian with the complete set of orthonormal eigenstates $|\alpha\rangle$, and $V(\boldsymbol{r},t)$ the periodic interaction.

The wave function ψ corresponding to a quasienergy state can be written as

$$\psi(\boldsymbol{r},t) = e^{-i\varepsilon t}\phi(\boldsymbol{r},t) \tag{A3}$$

where the quasienergy ε has a real value.

We define the operator $\mathcal{H}(\boldsymbol{r},t)$ as

$$\mathcal{H}(\boldsymbol{r},t) = H(\boldsymbol{r},t) - i\frac{\partial}{\partial t} \tag{A4}$$

verifying

$$\mathcal{H}\psi(\boldsymbol{r},t) = 0. \tag{A5}$$

If we substitute (A3) and (A4) in (A5), we obtain the eigenvalue equation for the operator $\mathcal{H}(\boldsymbol{r},t)$,

$$\mathcal{H}\phi_\gamma(\boldsymbol{r},t) = \varepsilon_\gamma\phi_\gamma(\boldsymbol{r},t). \tag{A6}$$

Due to the periodicity of the interaction, the function ϕ is also periodic with the same period [13] $\phi(\boldsymbol{r},t+2\pi/\omega) = \phi(\boldsymbol{r},t)$; thus the function can be expanded in a Fourier series,

$$\phi_\gamma(\boldsymbol{r},t) = \sum_{n=-\infty}^{n=\infty} A_n^\gamma(\boldsymbol{r})e^{-in\omega t}. \tag{A7}$$

A quasienergy state can then be expressed as

$$\psi_\gamma(\boldsymbol{r},t) = e^{-i\varepsilon_\gamma t}\phi_\gamma(\boldsymbol{r},t) = e^{-i\varepsilon_\gamma t}\sum_{n=-\infty}^{n=\infty} A_n^\gamma(\boldsymbol{r})e^{-in\omega t}. \tag{A8}$$

Note that if we replace the quasienergy ε_γ by $\varepsilon'_\gamma+m\omega$ and $\phi_\gamma(\boldsymbol{r},t)$ by $\phi'_\gamma(\boldsymbol{r},t)e^{im\omega t}$, Eq. (A6) is still verified, meaning

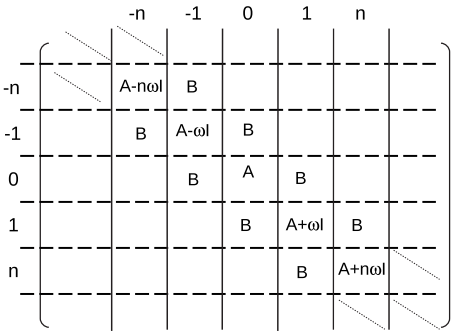

FIG. 8. Structure of Floquet matrix.

that ε'_γ and $\phi'_\gamma(\boldsymbol{r},t)$ are also an eigenvalue and eigenstate of the equation. However, the function ψ_γ in (A8) remains unchanged. That means that the states ψ_γ are physically equivalent if their quasienergies differ by $m\omega$. This property will be very useful for the line shape calculation.

2. Floquet Hamiltonian

The Floquet Hamiltonian is obtained by expanding the time-dependent wave function $\phi_\gamma(\boldsymbol{r},t)$ on the basis of functions $e^{-in\omega t}$. This is equivalent to considering quasienergy states as superpositions of stationary states with energies equal to $\varepsilon_\gamma + m\omega$.

The function $A_n^\gamma(\boldsymbol{r})$ in (A7) can be expanded on the basis of the eigenstates $|\alpha\rangle$ of H_0:

$$A_n^\gamma(\boldsymbol{r}) = \sum_\alpha a_{\alpha,n}^\gamma \langle \boldsymbol{r}|\alpha\rangle, \tag{A9}$$

where $\langle \boldsymbol{r}|\alpha\rangle = \varphi_\alpha(\boldsymbol{r})$ is an eigenfunction of H_0. We now note down the state $|\alpha n\rangle$ corresponding to the function $\varphi_\alpha(\boldsymbol{r})e^{-in\omega t}$.

An eigenfunction $\phi_\gamma(\boldsymbol{r},t)$ can then be expanded as

$$|\phi_\gamma\rangle = \sum_n \sum_\alpha a_{\alpha,n}^\gamma |\alpha n\rangle, \tag{A10}$$

where the states $|\alpha n\rangle$ form a complete orthonormal basis

$$\langle \beta m|\alpha n\rangle = \langle \beta|\alpha\rangle \lim_{\tau\to\infty} \frac{1}{\tau}\int_0^\tau e^{-i(n-m)\omega t}dt = \delta_{\alpha\beta}\delta_{nm}. \tag{A11}$$

Substituting Eq. (A10) into (A6) and operating with $\langle \beta m|$, we obtain

$$\langle \beta m|\mathcal{H}|\phi_\gamma\rangle = \varepsilon_\gamma \langle \beta m|\phi_\gamma\rangle, \tag{A12}$$

$$\sum_\alpha \sum_n [\langle \beta|H^{(n-m)}|\alpha\rangle - n\omega\delta_{\alpha\beta}\delta_{nm}]a_{\alpha,n}^\gamma = \varepsilon a_{\beta,m}^\gamma, \tag{A13}$$

with

$$H^{(n)} \equiv \lim_{\tau\to\infty} \frac{1}{\tau}\int_0^\tau H(\boldsymbol{r},t)e^{-in\omega t}dt \tag{A14}$$

We can identify in Eq. (A12) $\langle \beta|H^{(n-m)}|\alpha\rangle - n\omega\delta_{\alpha\beta}\delta_{nm}$ as the matrix element of the time-independent Floquet Hamiltonian,

$$\langle \beta m|H_F|\alpha n\rangle = \langle \beta|H^{(n-m)}|\alpha\rangle - n\omega\delta_{\alpha\beta}\delta_{nm}. \tag{A15}$$

If the interaction has a sinusoidal time dependence, the Floquet matrix has a tridiagonal block form as shown in Fig. 8. We see also that the matrix has a periodic structure with only the value $n\omega$, in the diagonal, varying from block to block. This structure leads to the following properties for the eigenvalues and eigenvectors:

$$\varepsilon_{\alpha n} = \varepsilon_{\alpha 0} + n\omega \tag{A16}$$

and

$$\langle \alpha, n+p|\varepsilon_{\beta,m+p}\rangle = \langle \alpha,n|\varepsilon_{\beta,m}\rangle, \tag{A17}$$

where $|\varepsilon_{\beta,m}\rangle$ stands for the eigenvector corresponding to the quasienergy eigenvalue $\varepsilon_{\beta,m}$.

[1] M. Baranger and B. Mozer, Phys. Rev. **123**, 25 (1961).
[2] E. A. Oks, St. Böddeker, and H. J. Kunze, Phys. Rev. A **44**, 8338 (1991).
[3] O. Renner, E. Dalimier, E. Oks, F. Krasniqi, R. Schott, and E. Förster, J. Quant. Spectrosc. Radiat. Transf. **99**, 439 (2006).
[4] N. C. Woolsey, J. Howe, D. M. Chambers, C. Courtois, E. Förster, C. D. Gregory, I. M. Hall, O. Renner, and I. Uschmann, High Energy Density Phys. **3**, 292 (2007).
[5] O. Renner, O. Peyrusse, P. Sondhauss, and E. Förster, J. Phys. B **33**, L151 (2000).
[6] V. P. Gavrilenko, A. Ya. Faenov, A. I. Magunov, T. A. Pikuz, I. Yu. Skobelev, K. Y. Kim, and H. M. Milchberg, Phys. Rev. A **73**, 013203 (2006).
[7] P. Audebert, R. Shepherd, K. B. Fournier, O. Peyrusse, D. Price, R. W. Lee, P. Springer, J.-C. Gauthier, and L. Klein, Phys. Rev. Lett. **89**, 265001 (2002).
[8] E. Oks, J. Phys. B **33**, L801 (2000).
[9] S. Alexiou, J. Quant. Spectrosc. Radiat. Transf. **71**, 139 (2001).
[10] C. Cohen-Tannoudji and S. Reynaud, J. Phys. B **10**, 345 (1977).
[11] O. Peyrusse, Phys. Scr. **56**, 371 (1997).
[12] J. H. Shirley, Phys. Rev. **138**, B979 (1965).
[13] S.-I Chu and D. A. Telnov, Phys. Rep. **390**, 1 (2004).
[14] U. Fano, Phys. Rev. **131**, 259 (1963).
[15] G. Ferrante, M. Zarcone, and S. A. Uryupin, Plasma Sources Sci. Technol. **10**, 318 (2001).
[16] A. B. Langdon, Phys. Rev. Lett. **44**, 575 (1980).
[17] S. B. Hansen and A. S. Shlyaptseva, Phys. Rev. E **70**, 036402 (2004).
[18] B. Talin, A. Calisti, J. W. Dufty, and I. V. Pogorelov, Phys. Rev. E **77**, 036410 (2008).
[19] E. Dufour, A. Calisti, B. Talin, M. A. Gigosos, M. A. González, T. del Río Gaztelurrutia, and J. W. Dufty, Phys. Rev. E **71**, 066409 (2005).
[20] H. R. Griem, M. Blaha, and P. C. Kepple, Phys. Rev. A **19**, 2421 (1979).
[21] E. W. Smith and C. F. Hooper, Phys. Rev. **157**, 126 (1967).
[22] L. A. Woltz and C. F. Hooper, Phys. Rev. A **30**, 468 (1984).
[23] L. A. Woltz and C. F. Hooper, Phys. Rev. A **38**, 4766 (1988).
[24] A. Calisti, F. Khelfaoui, R. Stamm, B. Talin, and R. W. Lee, Phys. Rev. A **42**, 5433 (1990).
[25] A. C. Kolb and H. Griem, Phys. Rev. **111**, 514 (1958).

[26] H. R. Griem, A. C. Kolb, and K. Y. Shen, Phys. Rev. **116**, 4 (1959).
[27] T. S. Ho, K. Wang, and Shih-I Chu, Phys. Rev. A **33**, 1798 (1986).
[28] O. Renner, P. Sauvan, E. Dalimier, C. Riconda, F. B. Rosmej, S. Weber, P. Nicolai, O. Peyrusse, I. Uschmann, S. Höfer, T. Kämpfer, R. Lötzsch, U. Zastrau, E. Förster, and E. Oks, in *Proceedings of the 19th International Conference on Spectral Line Shapes*, edited by M. A. Gigosos and M. A. González, AIP Conference Proceeding No. 1058 (AIP, Melville, NY, 2008), Vol. 15, p. 341.